



The effect of the likelihood function on the value of SHM extracted via sequential Bayesian updating

Antonios Kamariotis^a, Eleni Chatzi^b, and Daniel Straub^a

^aEngineering Risk Analysis Group, Technische Universität München, E-mail: {antonis.kamariotis, straub}@tum.de.

^bDepartment of Civil, Environmental and Geomatic Engineering, ETH Zurich, E-mail: chatzi@ibk.baug.ethz.ch.

ABSTRACT: This paper draws upon recent work of the authors (Kamariotis et al. 2022), which establishes a framework for the quantification of the Value of Information (VoI) from long-term vibration-based structural health monitoring (SHM). Within the proposed VoI analysis, a classical Bayesian model updating framework exploiting modal data identified from an Operational Modal Analysis (OMA) is implemented in a sequential setting to identify the parameters of stochastic deterioration models. Assumptions about the magnitude of the total prediction error in the OMA and the number of sensors can significantly affect the Bayesian updating results. In this work, we show that these effects can be quantified via the VoI.

1 INTRODUCTION

Widespread adoption of SHM systems on real-world structures and infrastructure systems is hampered by the lack of convincing demonstrations on how realistic monitoring data can instigate optimal maintenance decisions over the life-cycle of a structure. Value of information (VoI) analysis offers a framework for quantifying and optimizing the effect of SHM systems on life-cycle costs (Pozzi & Der Kiureghian 2011, Straub 2014).

In this direction, the authors have recently presented a preposterior Bayesian decision analysis tailored for quantifying the value of long-term vibration-based SHM (Kamariotis et al. 2021, 2022). In the proposed methodology, dynamic acceleration data are sampled at different time instances over the life-cycle of the structure and subsequently fed into an OMA procedure (Peeters & De Roeck 1999) to identify the modal data, i.e., system eigenfrequencies and mode shape displacements at the sensor locations. A classical Bayesian

model updating (BMU) framework (Simoen et al. 2015), which relies on the OMA-identified modal data, is implemented in a sequential setting to identify the damage evolution at potential damage locations. This subsequently leads to sequential updating of the estimated reliability of the system, and in turn allows for life-cycle optimization via use of a heuristic reliability threshold that triggers a repair action on the deteriorating structure.

Within the BMU framework, prior to installing the monitoring system, usually little (if anything) is known about the structure or magnitude of the total prediction error when constructing the likelihood function. Furthermore, the choice of the number and positions of employed sensors on the structure is important, especially in cases when damage localization is desired. This has motivated the authors to look at these assumptions and choices from the VoI perspective.

The mathematical details of the described VoI analysis will not be presented in this paper, and the interested reader is referred to



(Kamariotis et al. 2022). Herein, we demonstrate the VoI analysis via adoption of a numerical benchmark (Tatsis & Chatzi 2019), established as part of COST Action TU1402. It consists of a simulator for creating dynamic response measurement samples from a two span bridge system subject to corrosion deterioration in two hotspot locations over its lifespan. Using this case study, we compute the VoI that one obtains with the SHM i) for different assumptions about the magnitude of the total prediction error, ii) for different number of accelerometers uniformly distributed along the structure.

2 BAYESIAN MODEL UPDATING

2.1 Bayesian formulation

A vector $\theta \in \mathbb{R}^d$ contains all the d random variables (RVs) driving the uncertainty in the employed stochastic structural deterioration models. We employ a classical BMU framework in a sequential setting, which aims at sequentially inferring the parameters θ given noisy OMA-identified modal eigenvalues $\tilde{\lambda}_{t_m} = (2\pi\tilde{f}_{t_m})^2$ and mode shape vector components $\tilde{\Phi}_{t_m} \in \mathbb{R}^{N_s}$ at the N_s degrees of freedom (DOFs), which correspond to the sensor locations, where $m = 1, \dots, N_m$ is the number of the lower modes identified at time instance t . Typically, an OMA procedure, such as the Stochastic Subspace Identification (SSI) algorithm (Peeters & De Roeck 1999), can identify the m lower modal eigenvalues quite accurately, even when a relatively small number of acceleration sensors is deployed on the structure. However, the accuracy of the identification and the representation of the mode shape displacements depends heavily on the number of deployed sensors. Furthermore, quantities derived from the modal characteristics, as the mode shape curvatures $\tilde{K}_{t_m} \in \mathbb{R}^{N_s}$, are shown to enhance the damage localization capabilities of the BMU framework. For a successful derivation of the mode shape curvatures via a finite difference scheme, a dense arrangement of the accelerometers is required.

A linear finite element (FE) model, parameterized with θ , is employed for obtaining the FE model-predicted modal eigenvalues $\lambda_{t_m}(\theta)$ and mode shape displacements $\Phi_{t_m}(\theta)$, or mode shape curvatures $K_{t_m}(\theta)$.

The aim of the BMU framework is the estimation of parameters θ , and their uncertainty, such that the FE model predicted modal quantities best match the OMA-identified modal data. Long-term vibration-based SHM is supposed to provide sensor measurement data in a continuous fashion, therefore we are interested in a sequential implementation of the BMU framework. The goal is to learn at any time step t_i the posterior distribution of θ given all measurement data up to time t_i , i.e. the distribution $\pi_{\text{pos}}(\theta | \tilde{\lambda}_{1:i}, \tilde{\Phi}_{1:i})$. Applying Bayes' rule, this is proportional to the likelihood function $L(\theta; \tilde{\lambda}_{1:i}, \tilde{\Phi}_{1:i})$ multiplied with the prior probability density function (PDF) of the model parameters $\pi_{\text{pr}}(\theta)$:

$$\pi_{\text{pos}}(\theta | \tilde{\lambda}_{1:i}, \tilde{\Phi}_{1:i}) \propto L(\theta; \tilde{\lambda}_{1:i}, \tilde{\Phi}_{1:i}) \pi_{\text{pr}}(\theta) \quad (1)$$

The measurement uncertainty, including random measurement noise and variance or bias errors in the OMA procedure, and the model uncertainty, which together constitute the total prediction error (Simoen et al. 2015), have to be taken into account when constructing the likelihood function. The total prediction error for the eigenvalues and the mode shape vectors (accordingly for the mode shape curvatures), are in most state-of-the-art works formulated as follows:

$$\eta_{\lambda_{t_m}} = \tilde{\lambda}_{t_m} - \lambda_{t_m}(\theta) \in \mathbb{R} \quad (2)$$

$$\eta_{\Phi_{t_m}} = \gamma_{t_m} \tilde{\Phi}_{t_m} - \Phi_{t_m}(\theta) \in \mathbb{R}^{N_s} \quad (3)$$

where γ_{t_m} is a normalization constant, which is computed as in equation (4). Γ is a binary matrix for selecting the FE degrees of freedom, which correspond to the sensor locations.

$$\gamma_{t_m} = \frac{\tilde{\Phi}_{t_m}^T \Gamma \Phi_{t_m}}{\|\tilde{\Phi}_{t_m}\|^2} \quad (4)$$



The eigenvalue prediction error is assumed to follow a Gaussian distribution with zero mean and standard deviation proportional to the measured eigenvalues:

$$\eta_{\lambda_m} \sim \mathcal{N}\left(0, c_{\lambda_m}^2 \tilde{\lambda}_{t_m}^2\right) \quad (5)$$

The mode shape prediction error vector is assumed to follow a multivariate Gaussian distribution with zero mean vector and diagonal covariance matrix, where all the N_s components in the vector η_{Φ_m} are assigned the same standard deviation, proportional to the L_2 -norm of the measurement vector:

$$\begin{aligned} \eta_{\Phi_m} &\sim \mathcal{N}(0, \Sigma_{\Phi_m}) \\ \Sigma_{\Phi_m} &= \text{diag}\left(c_{\Phi_m}^2 \left\| \gamma_m \tilde{\Phi}_m \right\|^2\right) \end{aligned} \quad (6)$$

Assuming statistical independence among the N_t modal data sets obtained at different time instances and among the m identified modes at time instance t , the likelihood function is written as:

$$\begin{aligned} L\left(\theta; \tilde{\lambda}_1 \dots \tilde{\lambda}_{N_t}, \tilde{\Phi}_1 \dots \tilde{\Phi}_{N_t}\right) = \\ \prod_{t=1}^{N_t} \prod_{m=1}^{N_m} N\left(\tilde{\lambda}_{t_m} - \lambda_{t_m}(\theta); 0, c_{\lambda_m}^2 \tilde{\lambda}_{t_m}^2\right) \\ N\left(\gamma_{t_m} \tilde{\Phi}_{t_m} - \Phi_{t_m}(\theta); 0, \Sigma_{\Phi_{t_m}}\right) \end{aligned} \quad (7)$$

The factors c_{λ_m} and c_{Φ_m} are assigned coefficients of variation, whose chosen values represent an assumed deviation on the nominal model-predicted values, as induced due to the total prediction error (Simoen et al 2015). Even if some researchers have attempted to partially quantify the magnitude of this total prediction error (Reynders et al 2016), in practical applications usually little is known about the structure or the magnitude of the total prediction error prior to installing a monitoring system. The choice of an uncorrelated zero mean Gaussian model for the errors can be justified from the maximum entropy principle, but in the experience of the authors, most published literature contains a rather heuristic and unjustified choice of the magnitude of the factors c_{λ_m} and c_{Φ_m} , which affects the BMU results.

2.2 Laplace approximation of the posterior

For details, the interested reader is referred to the work of Beck & Katafygiotis (1998). The main idea is that for globally identifiable cases, and for large enough number of experimental data, the posterior distribution can be approximated by a multivariate Gaussian distribution $N(\mu, \Sigma)$. The mean vector μ is set equal to the most probable value, or maximum a-posteriori (MAP) estimate, of the parameter vector, which is obtained by minimizing the negative logposterior:

$$\begin{aligned} \mu = \theta_{MAP} &= \arg \min_{\theta} (-\ln \pi_{\text{pos}}(\theta \mid \tilde{\lambda}, \tilde{\Phi})) = \\ &= \arg \min_{\theta} (-\ln L(\theta; \tilde{\lambda}, \tilde{\Phi}) - \ln \pi_{\text{pr}}(\theta)) \end{aligned} \quad (8)$$

and the covariance matrix Σ is equal to the inverse of the Hessian of the log-posterior evaluated at the MAP estimate.

3 LIFE CYCLE COST OPTIMIZATION

This section is meant to provide a brief, high-level description of the preposterior Bayesian decision analysis methodology that is used herein to quantify the VoI. It is presented in full mathematical and algorithmic detail in (Kamariotis et al. 2022).

We assume some prior stochastic model(s) to describe the deterioration evolution over the lifetime at specific hotspot locations of a given structure. We employ the following simple decision model: At every time step of the decision problem, one has to choose whether or not a repair action should be performed on the structure. A repair action has an associated cost, which is subject to discounting over the lifetime. The event of failure of the structure at a specific time step is also associated with a cost. The total life-cycle cost is equal to the total cost of repair and the risk of failure cost over the lifetime of the structure. We make the simplifying assumption that a repair action results in replacing the damaged components and bringing them back to the initial state, and that



no failure will occur after a repair. This repair can also be interpreted as a replacement. The final goal is to find the optimal time to perform the repair/replacement over the life-cycle of the structure.

How do we decide at every time step of the decision problem whether a repair is necessary? Given the knowledge on the stochastic parameters of the deterioration model(s), it is possible to compute the accumulated probability of failure over time, and the corresponding hazard rate (Straub et al 2020, Melchers & Beck 2017). At the time step when the hazard rate exceeds a predefined threshold, a repair action is necessary. How do we choose the value of this predefined threshold? Employing a heuristic-based solution of the LCC optimization problem (Bismut & Straub 2021), the threshold on the hazard rate actually becomes the heuristic parameter which we seek to optimize, which results in the optimal t_{repair} .

3.1 Value of Information

A prior decision analysis is based solely on prior knowledge of the stochastic deterioration parameters θ , which is used to estimate the lifetime probability of failure and the hazard rate. On this basis, we estimate the optimal expected total life-cycle cost via a heuristic-based optimization.

In a preposterior decision analysis, the SHM information is accounted for, thus updating our prior assumptions. The process is described as follows. We draw samples from the prior distribution of θ . Each realization of the vector θ corresponds to one specific realization of the deterioration model(s), describing the structural damage evolution over time. For each possible realization of the deterioration model(s), we simulate corresponding modal data that one would obtain at each time step from an operational modal analysis using SHM acceleration measurements. Using the continuously obtained actual SHM data, we perform Bayesian analysis to sequentially learn the different posterior distributions of θ . We then use the estimated posteriors of

θ to estimate the updated lifetime probability of failure and the hazard rate. We eventually solve the LCC optimization to obtain the optimal time to perform the repair action for this specific deterioration and monitoring data realization. This procedure is performed for all samples of θ , resulting in the optimal expected LCC in the preposterior case.

The VoI is then straightforwardly computed as the difference between the optimal expected LCC in the prior case and the preposterior case.

3.2 Value of Partial Perfect Information

In a hypothetical scenario, where a perfect SHM system is assumed, at every time instance one acquires perfect knowledge on the true value of the parameters θ of the deterioration models, and the optimal repair decision is found conditional on this perfect knowledge. Since the SHM system cannot measure the load acting on the system, this information is only partially perfect. It is much simpler to perform a Value of Partial Perfect Information (VPPI) analysis, and it can provide an upper limit to the value that the VoI may assume.

4 NUMERICAL INVESTIGATIONS

4.1 Numerical benchmark for SHM data creation on deteriorating structure

In Figure 1 we show the numerical benchmark that is employed as a simulator for creating dynamic response measurement samples from the two span-bridge system, which is subjected to deterioration due to corrosion in the bottom elements of each midspan. It is assumed that there are 24 deployed accelerometers measuring vertical accelerations. Since we are interested in application of SHM on an operational level, the absence of knowledge on the load is simulated by assuming a distributed Gaussian white noise excitation acting on the structure. A dynamic time history analysis of the model results in the measured vertical acceleration signals at the 24 locations. These are contaminated with

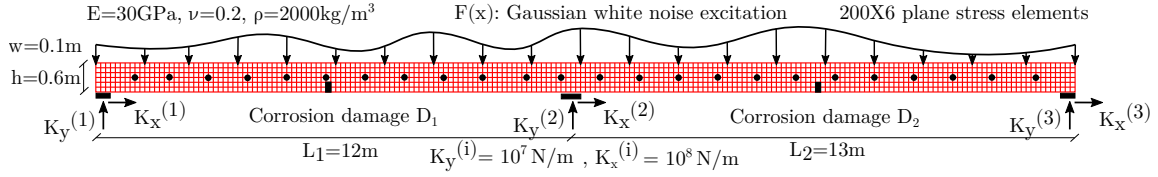


Figure 1: Bridge system subject to corrosion damage in two locations

Table 1: Parameters of the stochastic deterioration models

Parameters	Distribution	Mean	CV
A_1, A_2	Lognormal	0.506	0.4
B_1, B_2	Normal	0.5	0.15

noise, simulating sensor (measurement) error, and then fed into the SSI to obtain the m lower eigenvalues and mode shape displacements at the 24 sensor locations.

4.2 Deterioration models

We assume that the bridge structure is subjected to gradual deterioration from corrosion in the mid-section of both midspans (elements in black in Figure 1). At both locations, damage is introduced as a progressive reduction of stiffness at the bottom 2 elements of the FE mesh. The evolution of the stiffness reduction over the lifespan of the bridge is described by employing the damage model of equation (9). $E^{(0)}$ is the initial undamaged value of the Young's modulus, and $D_1(t)$, $D_2(t)$ are the deterioration models (reduction of stiffness) employed for each location. The random variables of the deterioration models are summarized in Table 1.

$$E_j(t) = E^{(0)} / (1 + D_j(t)) = E^{(0)} / (1 + A_j t^{B_j}),$$

$$j = 1, 2$$
(9)

4.3 Effect of the likelihood function on the BMU results

The FE model predicting the eigenvalues and mode shape displacements within the BMU process is the same FE model as the one in Figure 1 used for creating the synthetic noisy

monitoring data. Even though an artificial noise is added, the use of the same model partially neglects the model uncertainty. Nevertheless, this is a built-in feature of preposterior analysis.

For the depicted scenario of 24 accelerometers uniformly distributed along the structure, we can accurately identify the lower $N_m=6$ eigenvalues and mode shape displacements with the use of the SSI. Conditional on the good representation of the mode shape displacement vector that we can obtain with this dense sensor arrangement, a finite difference scheme is applied and the lower $N_m=6$ mode shape curvatures are obtained (Figure 2), which can be used in the likelihood function instead of the mode shape displacements.

It is assumed that the underlying "true" deterioration parameter values correspond to $A_1^* = 0.503$, $B_1^* = 0.459$, $A_2^* = 0.637$ and $B_2^* = 0.584$. For the "true" deterioration curves that these parameters define, we generate one set of OMA-identified modal data per year over the $T=50$ years of the lifetime, and using those we employ the sequential Bayesian deterioration model updating framework to learn the different posterior distributions of interest. In this simple example, the effect of environmental and operation variability on the structural properties are neglected.

4.3.1 Effect of the assumed total prediction error magnitude

The goal of this section is to illustrate the extent to which the assumed magnitude of the total prediction error, i.e., the choice of c_{λ_m} and c_{Φ_m} in the likelihood function, can affect the results of the Bayesian updating.

Figures 3, 4, 5 show the final posterior densities $\pi_{\text{pos}}(\theta | \tilde{\lambda}_{1:50}, \tilde{K}_{1:50})$ for each of the four

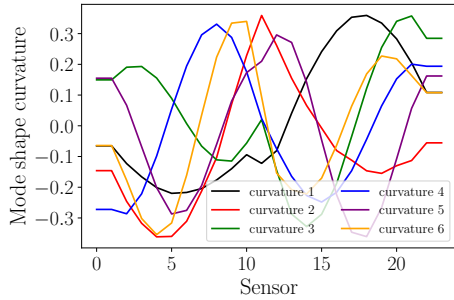


Figure 2: Mode shape curvatures in initial undamaged state

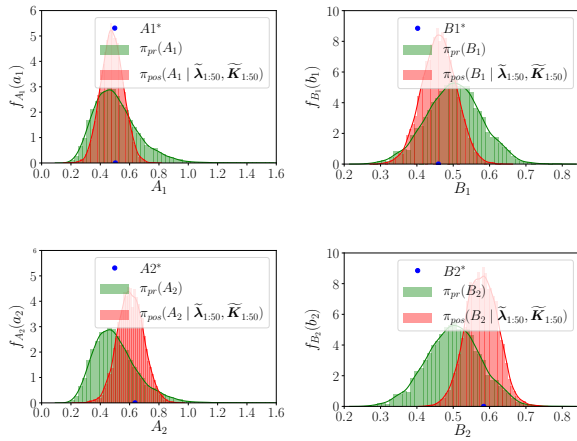


Figure 3: Final posteriors for $c_{\lambda m} = c_{\Phi m} = 2\%$, 24 sensors

uncertain variables of the two deterioration models (in red), together with the prior densities (in green), for three different choices of $c_{\lambda m}$ and $c_{\Phi m}$. One can directly observe that the results differ significantly among the three choices. For $c_{\lambda m} = c_{\Phi m} = 2\%$, the uncertainty in the posterior densities is reduced compared to the prior densities, and the posterior densities peak around the underlying "true" values for which the data was created. However, for $c_{\lambda m} = c_{\Phi m} = 5\%$ or 10% , the posterior densities that we obtain seem to be biased, i.e., they do not peak around the "true" values of the parameters, and the deterioration models one is learning do not correspond to the underlying "true" models. Since the posterior samples are eventually used within a structural reliability calculation, this means that also the estimate of the accumulated probability of failure and the hazard rate will have a large difference for the different choices of $c_{\lambda m} = c_{\Phi m}$, as shown in Figure 8.

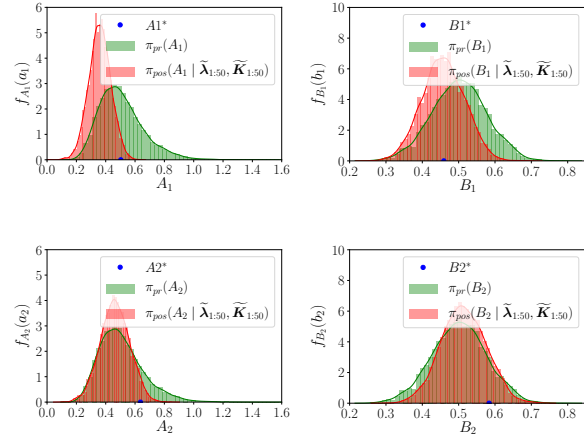


Figure 4: Final posteriors for $c_{\lambda m} = c_{\Phi m} = 5\%$, 24 sensors

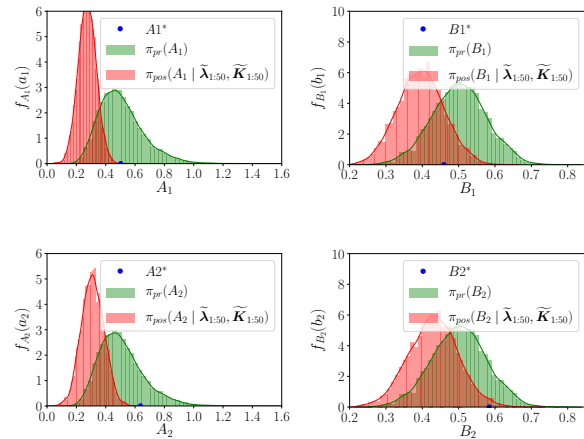


Figure 5: Final posteriors for $c_{\lambda m} = c_{\Phi m} = 10\%$, 24 sensors

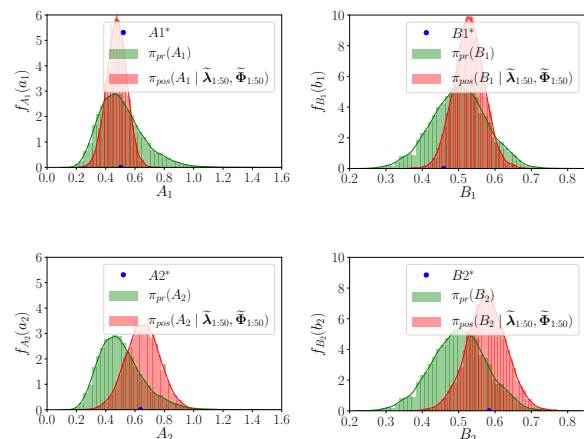


Figure 6: Final posteriors for $c_{\lambda m} = c_{\Phi m} = 2\%$, 8 sensors

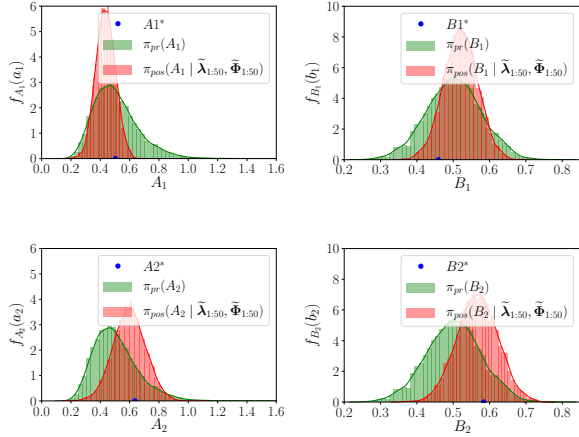


Figure 7: Final posteriors for $c_{\lambda m} = c_{\Phi m} = 2\%$, 16 sensors

4.3.2 Effect of the number of uniformly distributed sensors

The results of the previous section correspond to a case when 24 sensors are uniformly distributed along the length of the bridge structure. In that case, as can be seen in Figure 2, one can obtain a smooth representation of the mode shape curvatures, which is used in the likelihood function. However, when fewer sensors are available, it is no longer wise to extract the mode shape curvatures, since the finite difference scheme with a rather coarse sensor placement will not perform well. In that case, we use the mode shape displacements in our likelihood function for the BMU.

Figure 6 shows the final posterior densities obtained via the BMU framework for the case when only 8 sensors are uniformly distributed along the structure, while Figure 7 corresponds to the case of 16 sensors. Both results are obtained for $c_{\lambda m} = c_{\Phi m} = 2\%$. Comparing Figures 6, 7 to Figure 3, one can see the effect of the number of sensors on the performance of the BMU for detecting and localizing the damage at the two different deterioration hotspots. In Figure 8, the corresponding estimated hazard rate curves are shown.

Performing a VoI analysis for each of the three choices of the sensor placement, one can investigate the effect of this choice on the VoI result. Ultimately, such a parametric study can form the basis for optimal sensor placement.

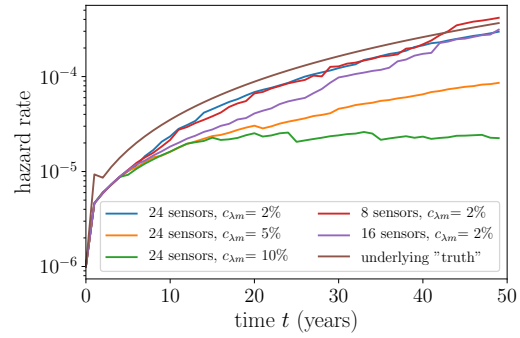


Figure 8: Hazard rate curves updated at each time step using the posterior distributions of the deterioration model parameters obtained via BMU for one "true" realization A_1^* , B_1^* , A_2^* and B_2^* .

Figures 3 - 7 show the posterior distributions of θ inferred via BMU using sampled modal data corresponding to one underlying "true" realization of the deterioration model parameters A_1^* , B_1^* , A_2^* and B_2^* . Within a VoI analysis, the posterior analysis via BMU has to be performed multiple times, for different sample realizations of the parameter vector θ .

4.4 Effect of the likelihood function on the VoI results

Finally, in this section we document the VPPI result and the different VoI results that we obtain for the various choices of the sensor placement and the assumed total prediction error magnitude.

In the context of the decision problem, we assume that the cost of failure is $\hat{c}_F = 10^7$ units and the cost of repair is $\hat{c}_R = 3.5 \times 10^4$ units, while the discount rate is 2%.

For the computation of the VoI, we draw 1000 samples of θ , which we use for executing both the prior and the preposterior decision analysis. In the preposterior case, for each of the θ samples, we create one continuous set of SSI-identified modal data, thus jointly sampling the system state space and monitoring data space.

Table 2 documents the optimal heuristic value and the optimal time to perform the repair, which minimize the total expected life-cycle cost in the prior decision analysis. The results of the preposterior decision analysis



for the different sensor arrangements and error magnitudes are shown in the following two subsections.

Table 2: Heuristic-based life-cycle optimization in the prior case.

w_0^*	t_{repair}^*
6.1×10^{-5}	21

4.4.1 Effect of the number of sensors on the VoI results

Table 3 documents the optimal value of the heuristic threshold w , which leads to an optimization of the total expected life cycle cost in the preposterior case, with Table 4 documenting the VPPI and VoI values for the three different numbers of uniformly distributed sensors. It is observed that the optimal heuristic threshold (the value of the hazard rate which instigates a repair action) takes larger values in the cases of fewer sensors. The VoI result yielded via the BMU process is highest for 24 sensors, and decreases when fewer sensors are deployed. Such a result would be expected. The coefficient of variation (CV) of the estimated mean value of the VoI also increases for fewer sensors, revealing the presence of larger noise in the estimation, when data from only few sensors are employed.

Table 3: Heuristic-based life-cycle optimization in the preposterior case ($c_{\lambda m}=c_{\Phi m}=2\%$). Different number of sensors.

sensors	w^*
24	1×10^{-4}
16	2.8×10^{-4}
8	3.9×10^{-4}

Table 4: Effect of the number of sensors on the VoI extracted via BMU ($c_{\lambda m}=c_{\Phi m}=2\%$). Different number of sensors.

VPPI (CV)	sensors	VoI (CV)	$\frac{VoI}{VPPI}$
7681 (2.6%)	24	4614 (5.3%)	60%
	16	2801 (13%)	37%
	8	2543 (16%)	33%

4.4.2 Effect of the assumed total prediction error magnitude on the VoI

Table 5 documents the optimal heuristic threshold value that we compute in the LCC optimization for the three different cases of error magnitude in the likelihood function used in the BMU. The optimal heuristic threshold that we obtain for $c_{\lambda m}=c_{\Phi m}=5\%$ and 10% drops compared to the case of $c_{\lambda m}=c_{\Phi m}=2\%$. This is in line with the observed behavior of the updated hazard rate curves that are shown in Figure 8 for the different cases.

Table 5: Heuristic-based life-cycle optimization in the preposterior case (24 sensors). Different values of $c_{\lambda m}=c_{\Phi m}$.

$c_{\lambda m}=c_{\Phi m}$	w^*
2%	1×10^{-4}
5%	5.5×10^{-5}
10%	2.65×10^{-5}

Table 6: Effect of the total prediction error magnitude on the VoI extracted via BMU (24 sensors). Different values of $c_{\lambda m}=c_{\Phi m}$.

VPPI (CV)	$c_{\lambda m}=c_{\Phi m}$	VoI (CV)	$\frac{VoI}{VPPI}$
7681 (2.6%)	2%	4614 (5.3%)	60%
	5%	4272 (6.8%)	55%
	10%	5489 (4.5%)	71%

The VoI results in Table 6 come at a surprise at a first glance. We showed in Section 4.3.1 that the choice of $c_{\lambda m}=c_{\Phi m}$ largely affects the BMU results, with the posterior estimates that we obtain being increasingly "off" as the magnitude of $c_{\lambda m}=c_{\Phi m}$ increases. Yet the VoI that we compute is large also for these cases. How can this be explained?

The posterior estimates obtained for $c_{\lambda m}=c_{\Phi m}=5\%$ and 10% seem to be characterized by a large bias. This bias seems to be present as a systematic error in all BMU analyses required within a preposterior Bayesian decision analysis. Our heuristic-based solution of the decision problem operates by optimizing the hazard rate threshold value, which instigates a repair action. The VoI analysis framework can compensate for this



completely systematic error that is present in the different posterior BMU analyses. In the end, by adjusting the optimal value of the heuristic threshold, the decisions on the optimal time to repair do not differ much between the different $c_{\lambda m}=c_{\Phi m}$ cases.

For demonstration purposes, we assume the following scenario, which is probably close to what would happen in practice: We assume that a decision on a repair is taken when the hazard rate exceeds a predefined threshold of 1×10^{-4} . This value is not subject to further optimization. Using this predefined threshold, we compute the expected total life-cycle cost in a prior decision analysis as well as in the different preposterior decision analyses. The VoI results yielded in this scenario are documented in Table 7. Here, it is observed that for this fixed threshold, the VoI resulting from a BMU analysis with large assumed values of the total prediction error is much smaller than the VoI result for lower values.

Table 7: Effect of the total prediction error magnitude on the VoI extracted via BMU (24 sensors) without an optimization of the heuristic threshold, which is set equal to 1×10^{-4} . Different values of $c_{\lambda m}=c_{\Phi m}$.

$c_{\lambda m}=c_{\Phi m}$	VoI
2%	5492
5%	4101
10%	539

5 CONCLUSIONS

This paper employs a preposterior Bayesian decision analysis framework for the quantification of the VoI yielded via adoption of vibration-based SHM on a deteriorating bridge structure. A key ingredient within this framework is the BMU, which aims at sequentially identifying the uncertain deterioration model parameters. It has been shown that the performance of the BMU in identifying and localizing structural deterioration is crucially affected by the employed likelihood function. The BMU leads to erroneous results for certain choices of the to-

tal prediction error magnitude in the likelihood function and - as expected - the BMU performance is decreasing when fewer sensors are deployed on the structure. The effect of these choices on the resulting VoI from SHM is quantified herein. The fewer the deployed sensors, the larger is the noise present in the damage identification and subsequently the lower is the VoI that results from the preposterior Bayesian decision analysis. Surprisingly, the heuristic-based solution of the decision problem compensates for what appears to be a consistent bias present in the BMU when the assumed magnitude of the total prediction error is large, and the resulting VoI is a large value, even when the posterior predictions are off.

ACKNOWLEDGEMENTS

The support of the TUM Institute for Advanced Study, Germany, with the Hans Fischer Fellowship is gratefully acknowledged.

REFERENCES

- Beck, J. & Katafygiotis, L. 1998. Updating models and their uncertainties. I: Bayesian statistical framework. *Journal of Engineering Mechanics* 124(4): 455-461.
- Bismut, E. & Straub, D. 2021. Optimal adaptive inspection and maintenance planning for deteriorating structural systems. *Reliability Engineering and System Safety* 215: 107891.
- Kamariotis, A., Chatzi, E. & Straub, D. 2022. Value of information from vibration-based structural health monitoring extracted via Bayesian model updating. *Mechanical Systems and Signal Processing* 166: 108465.
- Kamariotis, A., Straub, D. & Chatzi, E. 2021. Optimal maintenance decisions supported by SHM: A benchmark study. In: Chen, A., Ruan, X., Frangopol, D. M. [eds.] *Life-Cycle Civil Engineering: Innovation, Theory and Practice: Proceedings of the 7th International Symposium on Life-Cycle Civil Engineering. IALCCE 2020, Shanghai, Oct. 27-30, 2020.*
- Melchers, R., Beck, A. 2017. *Structural Reliability*



Analysis and Prediction, 3rd Edition, New York:
John Wiley & Sons.

- Pozzi, M. & Der Kiureghian, A. 2011. Assessing the Value of Information for long-term structural health monitoring. In: SPIE Conference on Health Monitoring of Structural and Biological Systems, San Diego, California, USA.
- Peeters, B. & De Roeck, G. 1999. Reference-based stochastic subspace identification for output-only modal analysis. *Mechanical Systems and Signal Processing* 13(6): 855-878.
- Reynders, E., Maes, K., Lombaert, G. & De Roeck, G. 2016. Uncertainty quantification in operational modal analysis with stochastic subspace identification: Validation and applications. *Mechanical Systems and Signal Processing* 66-67: 13-30.
- Simoen, E., De Roeck, G. & Lombaert, G. 2015. Dealing with uncertainty in model updating for damage assessment: a review. *Mechanical Systems and Signal Processing* 56: 123-149.
- Straub, D. 2014. Value of information analysis with structural reliability methods. *Structural Safety* 49: 68-80.
- Straub, D., Schneider, R., Bismut, E. & Kim, H. 2020. Reliability analysis of deteriorating structural systems. *Structural Safety* 82: 101877.
- Tatsis, K. & Chatzi, E. 2019. A numerical benchmark for system identification under operational and environmental variability. In: 8th International Operational Modal Analysis Conference: IOMAC 2019, Copenhagen, Denmark.